Organic Process Research & Development **2010,** *14,* 537–543

Selective Oxidation of Methyl Diphenyl Methyl Mercapto Acetate to Methyl Diphenyl Methyl Sulfinyl Acetate Using a Novel Catalyst UDCaT-3†

Ganapati D. Yadav,* S. Subramanian, and Haresh G. Manyar

Department of Chemical Engineering, Institute of Chemical Technology (ICT), University of Mumbai, Matunga, Mumbai - 400 019, India

Abstract:

The synthesis of modafinil involves oxidation of methyl diphenyl methyl mercapto acetate (MDMMA) selectively to methyl diphenyl methyl sulfinyl acetate (MDMSA). The existing industrial process involves oxidation of the sulfide derivative with hydrogen peroxide in the presence of acetic acid as the solvent. If the temperature is not controlled, this reaction, being exothermic, involves the formation of the sulfone derivative also to some extent. The reaction also generates an effluent, which is corrosive and hazardous. This paper deals with the application of a new heterogeneous catalyst prepared in our laboratory, UDCaT-3, a ternary oxide of manganese and vanadium, for the oxidation of MDMMA with hydrogen peroxide in methanol as the solvent. The reaction was found to give the product sulfoxide selectively. A theoretical model was employed for the analysis of this solid−liquid slurry reaction, and effects of various parameters on the rate of reaction were evaluated. There was no effect of the external or of the internal mass transfer resistance on the rate of reaction, and the reaction was found to be intrinsically kinetically controlled, and the kinetic parameters were established.

Introduction

In the pharmaceutical industry syntheses of various drugs and their intermediates involve oxidations of the sulfide group to either the sulfoxide or the sulfone. The use of sulfoxides as key intermediates for drug synthesis has drawn increasing interest in recent years. Therefore, new methods for the preparation of sulfoxides continue to be developed.[1−3] The standard methods involve oxidation of organic sulfides by a number of methods and using a variety of oxidizing agents and catalysts. The most common reagent is hydrogen peroxide alone or in the presence of various catalysts.[4] However, the major difficulty encountered in these reactions is overoxidation to sulfones. As a result, there is an imperative need to develop alternative catalysts for selective oxidations. In continuation with the long-lasting interest in the area of selective oxidations, we herein explore the possibility of developing a selective oxidation methodology with the emphasis towards selectively obtaining sulfoxide from the oxidation of the sulfide group.[5−7]

The intermediate, methyl diphenyl methyl sulfinyl acetate (MDMSA), is prepared by oxidizing methyl diphenyl methyl mercapto acetate (MDMMA) in the presence of alkali with hydrogen peroxide, and then esterifying the product.[8] This process gives rise to effluents, which are costly to treat. Many methods are reported for selective conversion of sulfides to sulfoxides in recent years. Oxo(salen)chromium(V) complexes have been used by Sevvel and others.[9] Selective sulfoxidation has been carried out by manganese dioxide catalyzed with sulfuric acid/silica gel by Firouzabadi and others[10] Another method involves the use of calcium hypochlorite and moist alumina.[11] All these methods use either hazardous reagents or those catalysts, which are not easily recoverable.

Newer methods were developed to attain the required selectivities by varying the type of catalyst used and the reaction conditions. In one method, the reaction was carried out with hydrogen peroxide/selenium oxide system.[12] DiFuria and Modene have reported vanadium(V)-catalyzed oxidation of sulfides in alcohol solvents using hydrogen peroxide.[13] The use of hydrogen peroxide in the presence of aromatic seleninic acid for this facile, selective oxidation has also been reported.[14]

Heterogeneous and homogeneous catalysis in liquid- and vapor-phase oxidation processes can be considered on the basis of common mechanistic principles. However, the fundamental chemical steps are essentially the same whether the oxidation occurs in the coordination sphere of a soluble complex or on the adsorbed metal-containing surface.

This work is concerned with a method which uses a simple inexpensive oxidizing agent i.e. hydrogen peroxide in the presence of a novel redox catalyst, UDCaT-3 (the acronym is derived from University Department of Chemical Technology, UDCT, Mumbai). The catalyst was recovered and reused.

† Institute of Chemical Technology (ICT) is formerly the University of Mumbai Institute of Chemical Technology (UICT), now a separate university.

* Tel: 91-22-2410-2121, Fax: 91-22-2414-5614, E-mail: gdyadav@yahoo.com, gd.yadav@ictmumbai.edu.in.

(1) Ho, T. L.; Ho, H. C.; Wong, C. M. *Synthesis* **1972**, 562.
(2) Barbieri, G.; Cinquini, M.; Colonna, S.; Montanari, V. *J. Chem. Soc. [C]* **1968**, 659.
(3) Louw, R.; Vermeerer, H. P. W.; van Asten, J. J. A.; Ultee, W. J. *J. Chem. Soc., Chem. Commun.* **1976**, 496.
(4) Hardy, F. E.; Speeleman, P. R. H.; Ronson, P. *J. Chem. Soc. [C]* **1969**, 2334.
(5) Manyar, H. G.; Chaure, G. S.; Kumar, A. *Green Chem.* **2006**, *8*, 344.
(6) Manyar, H. G.; Chaure, G. S.; Kumar, A. *J. Mol. Catal. A: Chem.* **2006**, *243*, 244.
(7) Yadav, G. D.; Manyar, H. G. *Adv. Synth. Catal.* **2008**, *350*, 2286.
(8) Lafon, L. Ger. Pat. 2,642,511, 1977.
(9) Sevvel, R.; Rajagopal, S.; Srinivasan, C.; Alhaji, N. M.; Chellamani, A. *J. Org. Chem.*, **2000**, *65*, 3334.
(10) Firouzabadi, H.; Abbasi, M. *Synth. Commun.* **1999**, *29*, 1485. 9.
(11) Hirano, M.; Yakabe, S.; Itoh, S.; Clark, J. H.; Morimoto, T. *Synthesis* **1997**, *10*, 1161.
(12) Drabowicz, J.; Mikolajczyk, M. *Synthesis* **1978**, 758.
(13) DeFuria, F.; Modene, G. In *Fundamentals of Research in Homogeneous Catalysis*; Tsutsui, M. , Ed.; Plenum Press: New York, 1979; Vol. 3, p 433.
(14) Reich, H. J.; Chen, F.; Peak, S. C. *Synthesis* **1978**, 299.

10.1021/op900304m
Published on Web 05/21/2010

Experimental Section

Chemicals and Catalysts. All chemicals were procured from firms of repute and used without further purification. MDMMA was prepared in our laboratory by an environmentally benign method described elsewhere.[1] Hydrogen peroxide (30% w/v aqueous) and methanol analytical grade (GC assay 99.9%) were obtained from M/s s.d. Fine Chem. Ltd., Mumbai India, UDCaT-3 catalyst was synthesized in our laboratory.

Catalyst Synthesis. UDCaT-3 catalyst was synthesized by using manganese oxide octahedral molecular sieve and cryptomelane as a scaffold. Cryptomelane was synthesized by a sol−gel route.[15] For synthesis of manganese vanadium ternary oxide $Mn(VO_3)_2$ over the cryptomelane framework through the solid-phase reaction, the vanadium precursor was adsorbed on the surface of cryptomelane by wet impregnation. A required amount of ammonium metavanadate was dissolved in 25 mL of 1 M oxalic acid solution. This precursor solution was then added to cryptomelane (3 g), and the temperature was raised to 65 °C. The mixture was stirred continuously until it was nearly dry. The product so obtained was further dried at 120 °C for 10 h, crushed to a powder form, and subsequently calcined at 450 °C for 6 h to get a brown-colored powder. During the calcination, the two oxides of vanadium (V_2O_5) and manganese (cryptomelane) underwent solid-state reaction to give manganese−vanadium ternary oxide. The formation of $Mn(VO_3)_2$ over a cryptomelane framework, during the solid-state interaction between manganese and vanadium oxides was studied by powder X-ray diffraction method. This material is named UDCaT-3.

Catalyst Characterization. UDCaT-3 was characterised by X-ray diffraction (XRD), surface area and pore size measurements, electron spin resonance (ESR), infrared (IR) and transmission electron microscopic (TEM) analyses. The X-ray scattering measurements were done with Cu Kα radiation by using a Siemens D 500 diffractometer. The scattered intensities were collected from 10 to 60° (2θ) by scanning at 0.025° (2θ) steps. Surface area, pore volume, and pore sizes were calculated from BET nitrogen adsorption/desorption isotherms obtained at liquid nitrogen temperature by using Micromeritics ASAP 2010 analyser. Transmission electron microscopy was carried out on a Philips CM 200 transmission electron microscope operating at 200 kV. Images were recorded on film. FTIR spectra were recorded by using a Perkin-Elmer Paragon 500 FT-IR spectrometer.

Reaction Procedure. The reaction was carried out in a cylindrical glass vessel of 150-mL capacity equipped with baffles and a turbine stirrer. The assembly was kept in an isothermal bath at a predetermined temperature and mechanically stirred at a known speed with an electrical motor. Predetermined quantities of reactants and solvent were added to the reactor, and the temperature was raised to the desired value. The catalyst was added when the temperature reached the set value. A typical reaction consisted of 0.01 mol MDMMA and 0.035 mol of hydrogen peroxide with a catalyst loading of 0.022 g/cm^3 at 30 °C. The reaction was carried out in methanol as the solvent with volume made up to 45.0 mL, at a speed of agitation of 1200 rpm. A zero time sample was collected, and sampling was done periodically to get concentration−time profiles of reactants and product.

(15) Duan, N.; Suib, S. L.; O'Young, C.-L. *Chem. Commun.* **1992**, 1213.

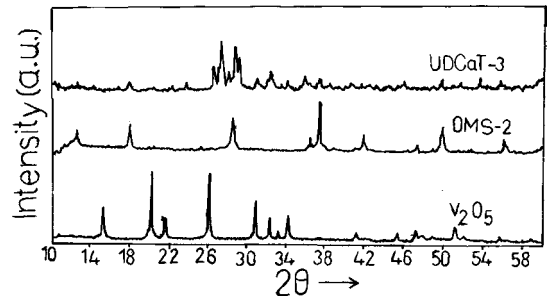

Figure 1. **X-ray diffraction patterns.**

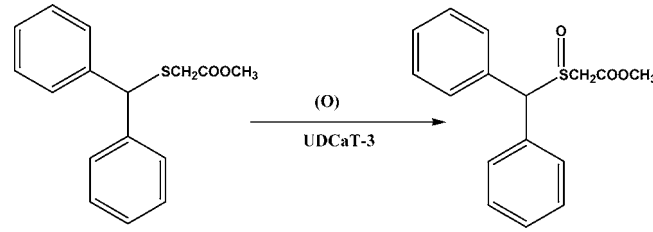

MDMMA **MDMSA**

Analysis. After filtration of the catalyst, the reaction mixture was analyzed. The reaction was monitored by instrumental analysis. The instrumental analysis was carried out by high performance liquid chromatography (HPLC) (Tosoh, UV-8010) at ambient temperature. The Merck 50983 column with a stationary phase of Lichrospher 100 RP-18, particle size 5 μm, prepacked on a 250 mm × 4 mm ID with Tosoh UV-8010 detector set at 230 nm was used for MDMMA and MDMSA. The eluent used for the analysis was HPLC grade methanol and deionized water in the ratio of 4:1 with a flow rate of 1.0 mL/min. Pure samples of the reactants and products and their synthetic mixtures were used to calibrate the chromatograms. For isolation of product, the catalyst was filtered off and methanol removed from the reaction mixture by using a rotovac. The product was isolated by standard procedures and characterized by infrared spectroscopy, IR (Perkin-Elmer). The product was purified by crystallization.

Results and Discussion

Catalyst Characterization. UDCaT-3 was thoroughly characterized by X-ray diffraction, volumetric (N_2 adsorption−desorption) and TEM analyses, and electron spin resonance (ESR) and framework IR spectroscopies. UDCaT-3 catalyst showed sharp X-ray diffraction peaks (Figure 1) with the presence of a mixed phase of cryptomelane and manganese−vanadium ternary oxide, $Mn(VO_3)_2$ with the 2θ values matching the reported data of cryptomelane[16] and the corresponding (*hkl*) values are (1 0 1), (0 0 2), (3 0 1), (2 1 1), (3 1 0), (1 1 4), and (6 0 0) at 2θ values of 12.7, 18.0, 28.7, 37.4, 41.8, 50.0, 55.3°. X-ray diffraction patterns of UDCaT-3 showed the presence of characteristic peaks of the ternary oxide, $Mn(VO_3)_2$ at 2θ values of 27.433 and 29.26°. The TEM of cryptomelane and UDCaT-3

(16) Database of Powder Diffraction Patterns: JCPDS: 34-168; International Centre for Diffraction Data [Joint Committee on Powder Diffraction Standards (JCPDS)]: Newtown Square, PA, 1994.

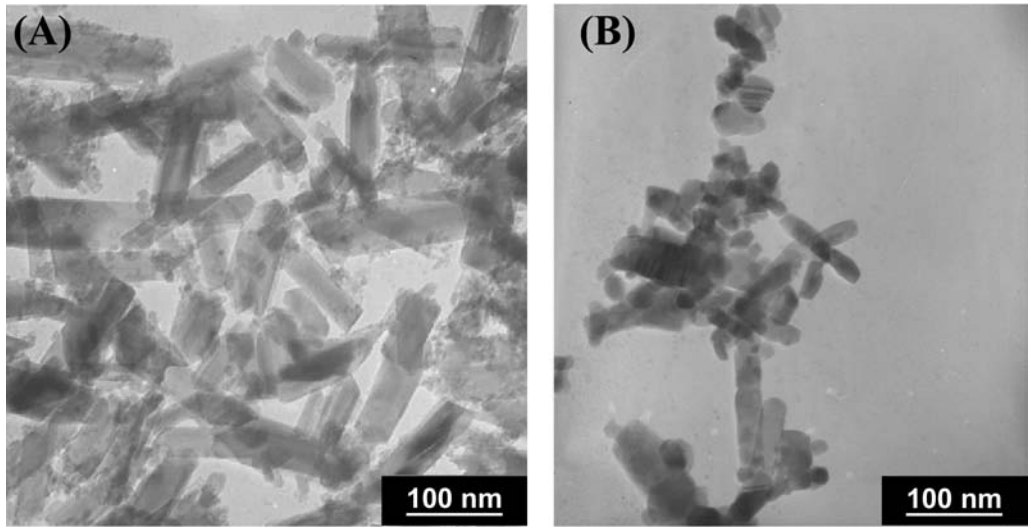

Figure 2. **TEM of (A) cryptomelane and (B) UDCaT-3.**

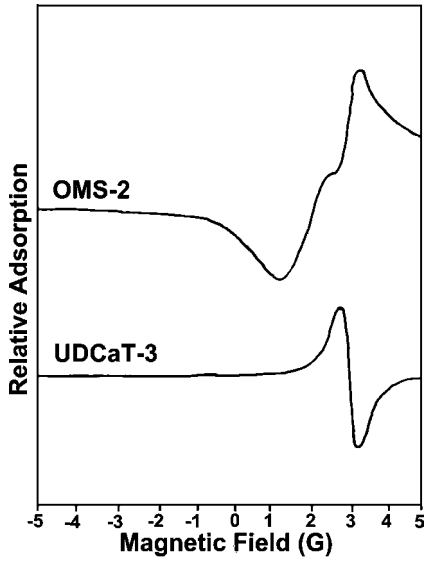

Figure 3. **ESR spectra of cryptomelane and UDCaT-3.**

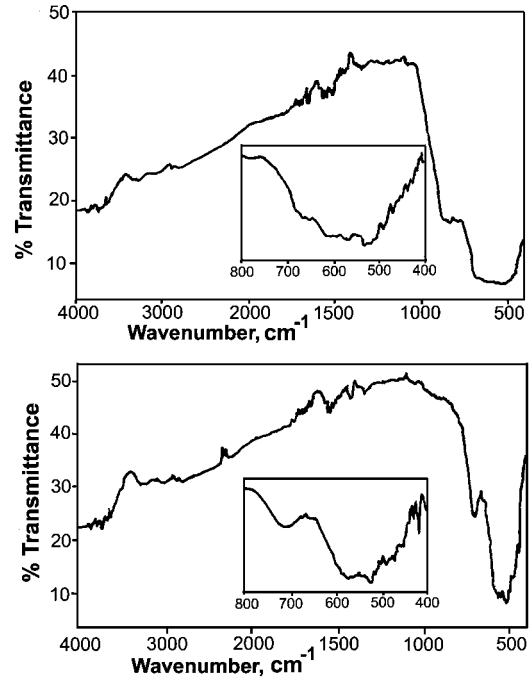

Figure 4. **IR spectrum of (A) cryptomelane and (B) UDCaT-3.**

are shown in Figure 2. They show the presence of mixed phases of the tunnel structure of cyptomelane and new $Mn(VO_3)_2$ ternary oxide particles finely dispersed on the rodlike morphology of cryptomelane. The size of cryptomelane crystals was observed to decrease which can be attributed to the solid-state reaction with V_2O_5 crystallites. UDCaT-3 catalyst showed a low BET surface area of 44 m^2/g with the pore volume of 0.37 cm^3/g. The pore size distribution of UDCaT-3 shows the presence of mesopores. The broad peak at about 25 Å is evidence of the presence of mesopores in UDCaT-3. Pore diameters are in the range of 16−64 Å with the maximum contribution of pore volume by mesopores in the range of 21−28 Å. The ESR measurements were used to study the chemical environments of Mn in the ternary oxide, $Mn(VO_3)_2$ in UDCaT-3. The ESR spectra of the UDCaT-3 and cryptomelane are shown in Figure 3. At room temperature, the ESR spectra of UDCaT-3 showed a broad, single line signal centered at $g = 2.0$, and no hyperfine or other resonances were found. Both Mn^{2+} and Mn^{4+} can give similar ESR spectra. However, Mn^{4+} shows g values less than 2. Mn^{2+} ions show purple to violet color, whereas Mn^{4+} ions are yellow colored.[5,17] The color of samples together with a g value at 2.0 suggest the presence of Mn^{2+} in an octahedral coordination structure. However, both the OMS-2 structure and $Mn(VO_3)_2$ have Mn ions at close distance, which may lead to antiferromagnetic interactions and a loss of the ESR signal. Thus, it was very difficult to conclude if the signal was obtained from Mn sites from OMS-2 framework or from Mn from $Mn(VO_3)_2$. IR spectra of UDCaT-3 and cryptomelane showed no prominent differences, other than enhanced intensities (Figure 4). Peaks at wave numbers 600 and 520 cm^{-1} are characteristics of cryptomelane. Peaks in the region 3400−3600 cm^{-1} belong to −OH groups of sorbed water molecules present in the framework. The bending vibration bands of water molecules were seen at ∼1640 cm^{-1}. The bands in the region of 700−760 cm^{-1} are due to vibrations of Mn−O bonds.

(17) Goldfarb, D. *Zeolites* **1989**, *9*, 509.

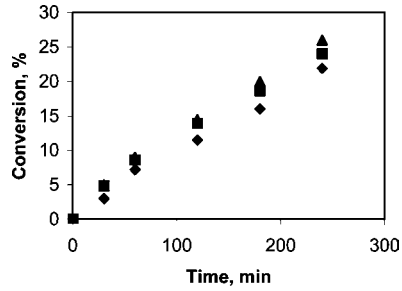

Figure 5. **Effect of speed of agitation: ◆ 800 rpm; ■ 1000 rpm; ▲ 1200 rpm; MDMMA: 0.01 mol; H_2O_2:0.0355 mol; catalyst loading:0.022 g/cm^3; temperature: 30 °C.**

Oxidation of MDMMA. In the liquid-phase oxidation of MDMMA performed in a batch process by using UDCaT-3 as a catalyst and aqueous hydrogen peroxide as the oxidizing agent, the corresponding sulfoxide MDMSA was the only product (100% selectivity). The reaction proceeded selectively to give MDMSA as the product, and no over-oxidation to sulfone was observed in the reaction. The catalytic activity of UDCaT-3 was compared with other catalysts/reagent reported in literature (Table 1). In comparison to various reagents or catalysts used in sulfide to sulfoxide oxidation, the methodology with UDCaT-3 catalyst and hydrogen peroxide was found to be the most promising and clean methodology with 100% selectivity to sulfoxide. It was thought desirable to study the influence of various reaction parameters under otherwise similar experimental conditions to establish the precise path of the reaction mechanism.

Table 1. **Comparison of the catalytic activity and selectivity of UDCaT-3**

no.	catalyst/reagent	yield %	reference
1	iodobenzene dichloride in aqueous pyridine	>80	2
2	acetyl nitrate or benzoyl nitrate	>90	3
3	vanadium pentoxide-hydrogen peroxide	50−80	4
4	oxo(salen)chromium(V) complexes in acetonitrile	30−95	9
5	manganese dioxide with H_2SO_4 on silica	50−85	10
6	calcium hypochlorite and moist alumina	45−95	11
7	UDCaT-3 with hydrogen peroxide	100	this work

Effect of Speed of Agitation. The reaction was carried out under at four different speeds of agitation (Figure 5). There was significant increase in the conversion from 800 to 1200 rpm, but it was almost constant beyond 1000 rpm. This indicated the absence of external solid−liquid mass transfer resistance beyond this point. All subsequent reactions were carried out with 1200 rpm as the speed of agitation.

For assessment of the external mass transfer resistance, the liquid-phase diffusivity values, D_{BA} (MDMMA in hydrogen peroxide) and D_{AC} (hydrogen peroxide in methanol), were calculated by using the Wilke−Chang equation.[18] The value of D_{BA}, diffusivity of B in A at 30 °C, was calculated as 5.295 × 10^{-5} cm^2/s and D_{AC} as 4.9452 × 10^{-5} cm^2/s.

(18) Reid, R. C.; Pransnitz, M. J.; Sherwood, T. K. *The Properties of Gases and Liquids*, 3rd ed.; McGraw-Hill: New York, 1977.

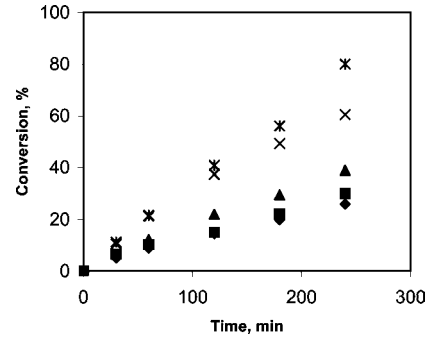

Figure 6. **Effect of catalyst loading: ◆ 0.0022 g/cm^3; ■ 0.0044 g/cm^3; ▲ 0.0066 g/cm^3; × 0.0088 g/cm^3; □ 0.011 g/cm^3; MDMMA: 0.01 mol; H_2O_2:0.0355 mol; speed of agitation:1200 rpm; temperature: 30 °C.**

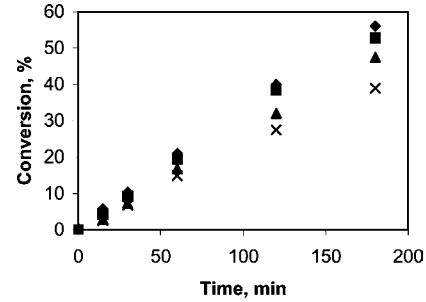

Figure 7. **Effect of various particle sizes: ◆ 45 μm; ■ 120 μm; ▲ 106.5 μm × 262 μm; MDMMA: 0.01 mol; H_2O_2:0.0355 mol; speed of agitation: 1200 rpm; temperature: 30 °C; catalyst loading: 0.0088 g/cm^3.**

The values of solid−liquid mass transfer coefficients $k_{SL\text{-}A}$, were calculated by assuming the Sherwood number, $Sh = (k_{SL}d_p)/D = 2$, where D is the bulk diffusivity of the concerned species. It should be noted that the actual Sherwood number could be much higher due to intense agitation, but for orders of magnitude calculation, it was safe to take the lowest Sherwood number. Thus, $k_{SL\text{-}A}$ was found as 1.177 × 10^{-2} cm/s for a particle size of UDCaT-3 of 0.009 cm. The value of a_P, particle surface area per unit liquid volume, was calculated from

$$a_P = \frac{6w}{(\rho_P d_P)} \text{ as } 1.544 \text{ cm}^2/\text{cm}^3 \quad (1)$$

Thus,

$$k_{SL-A}a_P[A_0] = 4.034 \times 10^{-6} \text{ g·mol·cm}^{-1}\text{·s}^{-1} \quad (2)$$

and

$$k_{SL-B}a_P[B_0] = 1.320 \times 10^{-5} \text{ g·mol·cm}^{-1}\text{·s}^{-1} \quad (3)$$

Thus, a typical initial rate of reaction was calculated as 1.0 × 10^{-8} g·mol·cm^{-3}·s^{-1}. Therefore,

$$\frac{1}{\eta k_{R_2} w[A_0][B_0]} \gg \frac{1}{k_{SL-A}a_P[A_0]} \text{ and } \frac{1}{k_{SL-B}a_P[B_0]} \quad (4)$$

i.e. 9.428 × 10^7 ≫ 2.478 × 10^5 and 7.5749 × 10^4.

The above inequality demonstrates that there is an absence of resistance due the solid−liquid external mass transfer, and

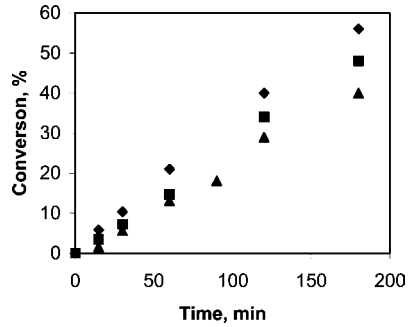

Figure 8. **Effect of different mole ratios: ◆ 1:3.5; ■ 1:2.6; ▲ 1:1.8; MDMMA: 0.01 mol; H_2O_2:0.0355 mol; speed of agitation: 1200 rpm; temperature: 30 °C; catalyst loading: 0.0088 g/cm^3; particle size: 45 μm.**

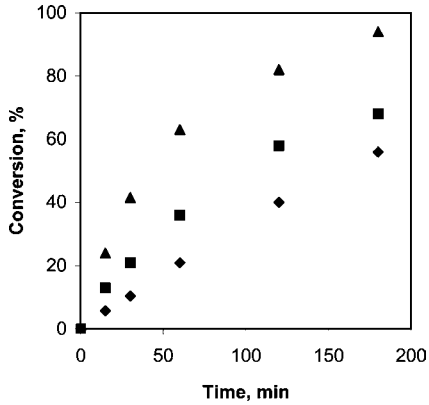

Figure 9. **Effect of temperature: ◆ 30 °C; ■ 40 °C; ▲ 50 °C; DPMMA: 0.01 mol; methanol: 1.5 mol; speed of agitation: 1000 rpm; catalyst loading: 0.02 g/cm^3; particle size: 120 μm; H_2O_2: 0.0355 mol.**

the rate may be either surface reaction controlled or intraparticle diffusion controlled.

Effect of Catalyst Loading. The reactions were conducted at four different catalyst loadings (Figure 6), in the range of 0.0022−0.011 g/cm^3. The conversion increased with increasing catalyst loading which was due to a proportional increase in the amount of sites and surface area, but beyond a loading of 0.0088 g/cm^3, there was no appreciable change in the reaction rates The catalyst loading of 0.0088 g/cm^3 was chosen for subsequent reactions to facilitate a proper kinetic study.

Effect of Particle Sizes. The effect of particle size on the conversion was studied in the range of 45 μm to 262 μm. An increase in the conversion was found as the particle size decreased from 262 μm to 120 μm (Figure 7), and no appreciable change was found as particle size further decreased from 120 to 45 μm. Below a particle size of 120 μm there was no resistance to intra particle diffusion, which was confirmed by using the Wiesz−Prater criterion. According to the Wiesz−Prater criterion, the dimensionless parameter $\{C_{wp} = -r_{obs}\,\rho_p\,R_p^2/D_e\,[C_A]\}$ which represents the ratio of the intrinsic reaction rate to the intraparticle diffusion rate, can be evaluated from the observed rate of reaction, the particle radius (R_p), effective diffusivity of the limiting reactant (D_e) and concentration of the reactant at the external surface of the particle. The effective diffusivity of MDMMA (D_e) inside the pores of the catalyst was obtained from the bulk diffusivity (D_{BA}) calculated as 6.71×10^{-6} cm^2 s^{-1}, porosity (ε) taken as 0.38, and tortuosity

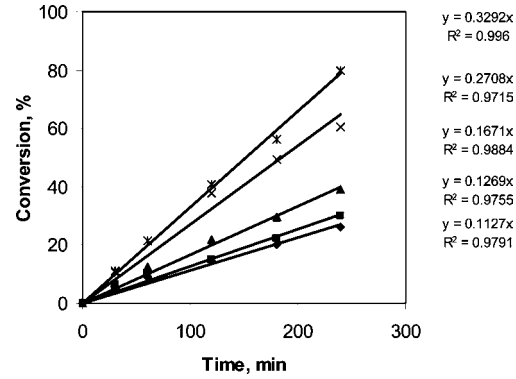

Figure 10. **Validation of the proposed kinetic model from the plot of X_A vs t for various catalyst loadings obtained from the experimental data: ◆ 0.0022 g/cm^3; ■ 0.0044 g/cm^3; ▲ 0.0066 g/cm^3; × 0.0088 g/cm^3; □ 0.011 g/cm^3; MDMMA: 0.01 mol; H_2O_2:0.0355 mol; speed of agitation: 1200 rpm; temperature: 30 °C.**

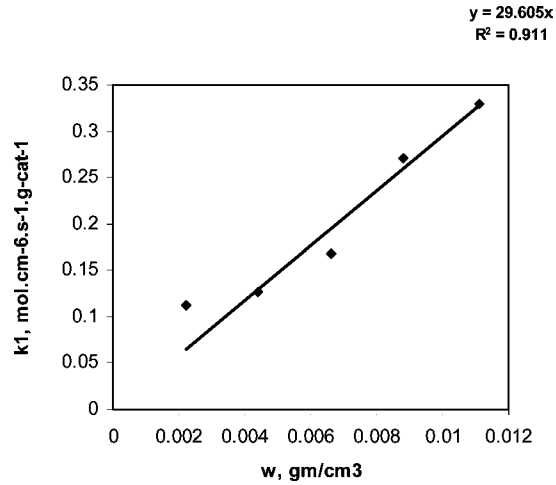

Figure 11. **Plot of k_1 vs catalyst loading.**

(τ) as 3.0, where $D_e = D_{BA} \cdot \varepsilon/\tau$. In the present case, the value of C_{WP} was calculated as for the initial observed rate and was found to be 6.52×10^{-5}; therefore, the reaction is intrinsically kinetically controlled. Further proof of the absence of intraparticle diffusion resistance was obtained through the study of the effect of temperature.

Effect of Different Mole Ratios. The effect of mole ratio was studied at MDMMA to hydrogen peroxide ratios of 1:1.8 to 1:3.5, keeping the total volume of the reaction mass constant at 45.0 mL with methanol. The catalyst loading was kept at 0.0088 g/cm^3. The conversion was found to be the maximum at the ratio of 1:3.5 (Figure 8). The mole ratio was kept at 1:3.5 for the remaining experiments.

Effect of Temperature. The reaction was carried out at 30, 40, and 50 °C (Figure 9) to study the effect of temperature on the conversion of MDMMA. It was found that the conversion increased substantially with increase in temperature. This also proves the absence of intraparticle resistance at the particle size of 120 μm, and the reaction is intrinsically kinetically controlled.

Mechanism. The reaction can be described by Mars van Krevelen mechanism. In this mechanism, the lattice oxygen from the tunnel structures enters the desorbable products. As the tunnel structure is depleted consequently, it is then replenished by oxygen from hydrogen peroxide. Thus it can say that

oxygen is not simply added to the reactant molecule but is first activated by transformation into lattice oxygen.[19,20] The structural framework of UDCaT-3 exhibits lattice oxygen vacancies in its tunnel structure. This composite catalyst works via redox mechanism known as Mars van Krevelen mechanism wherein lattice oxygen from the tunnel structures enters the desorbable products.[21−23] The step of oxygen depletion and the subsequent replenishment makes it a regenerative catalyst. The catalyst has two types of sites, S_1 and S_2, where S1 is the lattice oxygen vacancy in the tunnel structure and S_2 is the site adjacent to S_1. The following steps are proposed to be taking place in the Mars van Krevlen mechanism.

(i) H_2O_2 is adsorbed at the lattice vacancies in the tunnel structure of UDCaT-3 (S_1) catalyst. Eventually, this is both an adsorption and an equilibrium step. This step is expressed as

$$H_2O_2(aq) + \text{UDCaT-3} \xrightarrow{k_1} H_2O_2\cdot\text{UDCat-3} \qquad (5)$$

(ii) H_2O_2 adsorbed on UDCaT-3 catalyst is activated and decomposed to water, and atomic oxygen remains in the framework of UDCaT-3 catalyst as a framework lattice oxygen.

$$H_2O_2\cdot\text{UDCat-3} \rightarrow H_2O + \text{O}\cdot\text{UDCaT-3} \qquad (6)$$

(iii) Adsorption of substrate B on the adjacent site (S_2)

$$B + S_2 \rightleftarrows BS_2 \qquad (7)$$

(iv) Surface reaction between the adsorbed species:

$$OS_1 + BS_2 \rightarrow PS_2 + S_1 \qquad (8)$$

Kinetics. The inspection of the conversion against time plots in all cases shows that the reaction is zero order reaction in both reactants. That means there are two different sites due to strong adsorption of both the reactants. For oxidation, the oxygen comes from the catalyst and is then replaced by the oxidant. Since H_2O_2 is taken in excess, the rate is much faster. There is a parallel reaction of H_2O_2 decomposition on the metal oxide surface and a substantial part of H_2O_2 added is decomposed. Hence, on increasing the H_2O_2 mole ratio, more H_2O_2 participates in the oxidation reaction, and the overall reaction rate increases.

The substrate sits on a site adjacent to the O of the catalyst. Total site concentrations $= C_{S1} + C_{S2}$. The rate is given by:

$$r_A = \frac{-dC_A}{dt} = kw\left(\frac{K_1C_1}{1 + K_1C_1}\right)\left(\frac{K_2C_2}{1 + K_2C_2}\right) \qquad (9)$$

When both are strongly adsorbed, the terms in the denominator individually become greater than one. Thus,

$$r_A = \frac{-dC_A}{dt} = kw \qquad (10)$$

w is catalyst loading. So in terms of conversion, it is

$$r_A = \frac{-dC_A}{dt} = C_{A_0}\frac{dX_A}{dt} = kw \qquad (11)$$

The above equation can be integrated as:

$$X_A = \frac{kwt}{C_{A_0}} \qquad (12)$$

Thus the conversion of the substrate is directly proportional to time. All the plots show that the above equation is obeyed where the slope is

$$\frac{kw}{C_{A_0}} = k_1 \qquad (13)$$

A plot of X_A vs t for various catalyst loadings is given in Figure 10. From this graph, the values of k_1 were determined.

A plot of k_1 against w, for catalyst loading in g/cm^3, was found to be a straight line, whose slope was $(k)/(C_{A_0})$ (Figure 11). The value of k calculated from the slope is 1.0965×10^{-4} mol·cm^{-6}·s^{-1}·g-cat^{-1}.

The above analysis shows that the experimental data fit the model very well.

The theory that is advocated here shows that the reaction follows zero-order kinetics (Figures 10 and 11), and the rate constant was found to be 1.0965×10^{-4} mol·cm^{-6}·s^{-1}·g-cat^{-1}.

Conclusions

The current synthesis of modafinil involves several polluting steps in the overall process. One of them is the oxidation of MDMMA selectively to MDMSA. This method of oxidation of MDMMA, with hydrogen peroxide in the presence of a novel redox catalyst UDCaT-3, proved to be very promising with high selectivity towards the sulfoxide product. A theoretical model was employed for the analysis of this solid−liquid slurry reaction, and effects of various parameters on the rate of reaction were evaluated. There was no effect of external or of internal mass transfer resistance on the rate of reaction. The reaction was found to be intrinsically kinetically controlled, and the kinetic parameters were established. The reaction follows an overall zero-order kinetics. The process is clean and green.

NOMENCLATURE

a_P	solid−liquid interfacial area (cm^2/cm^3 of liquid phase)
A	hydrogen peroxide
$[A_0]$	initial concentration of A in bulk liquid phase (mol/cm^3)
$[B_0]$	initial concentration of B in bulk liquid phase (mol/cm^3)
B	MDMMA

(19) Doornkamp, C.; Ponec, V. *J. Mol. Catal. A.* **2000**, *162*, 19.
(20) Zhou, H.; Shen, Y. F.; Wang, J. Y.; Chen, X.; O'Young, C.-L.; Suib, S. L. *J. Catal.* **1998**, *176*, 321.
(21) Mars, P.; van Krevelen, D. W. *Chem. Eng. Sci.* **1954**, *3* (Special Suppl.), 41.
(22) Mars, P.; Maessen, J. G. H. *Proceedings of the Third ICC, Amsterdam*; Elsevier: North Holland, Amsterdam, 1964; Vol. 1, p 266.
(23) Boreskov, G. K., Ed. *Catalysis: Science and Technology*; Springer: Berlin, 1982, Vol. 3, p 39.

C	methanol
C_A	concentration of A (mol/cm^3)
C_s	concentration of active sites on the catalyst surface (mol/g)
C_{wp}	Wiesz−Prater parameter
D	bulk diffusivity (cm^2/S)
d_p	diameter of catalyst particles (cm)
D_{AC}	diffusion coefficient of A in C (cm^2/s)
D_{BA}	diffusion coefficient of B in A (cm^2/s)
D_e	effective diffusivity of MDMMA (cm^2/s)
k_1	adsorption equilibrium constant for A
k_{SL}	solid−liquid mass transfer coefficient (cm/s)
MDMMA	methyl diphenyl methyl mercapto acetate
MDMSA	methyl diphenyl methyl sulfinyl acetate
r_{obs}	overall rate of reaction based on liquid-phase volume (mol cm^{-3} s^{-1})
R_p	radius of catalyst particle (cm)
S	catalyst active site
Sh	Sherwood number
w	catalyst loading (g/cm^3)

Greek symbols

ε	catalyst porosity
τ	tortuosity
ρ_p	density of catalyst particle (g/cm^3)

Acknowledgment

Thanks are due to the following for their support in carrying out research described in this paper: University Grants Commission, for Senior Research Fellowship to S.S., Senior Research Fellowship to H.G.M. under NMITLI programme of CSIR, New Delhi and Darbari Seth Professor Endowments to G.D.Y. He also thanks the R.T. Mody Distinguished Professor endowment for the Chair. Thanks are also due to the Michigan State University for hosting G.D.Y. as the Johansen-Crosby Visiting Chair Professor of Chemical Engineering during 2001-2002 which provided an excellent atmosphere for creative pursuits.

Received for review November 16, 2009.

OP900304M